

A proposed chemical scheme for HCCO formation in cold dense clouds

V. Wakelam^{1,2*}, J.-C. Loison^{3,4}, K. M. Hickson^{3,4}, M. Ruaud^{1,2}

¹ *Univ. Bordeaux, LAB, UMR 5804, F-33270, Floirac, France.*

² *CNRS, LAB, UMR 5804, F-33270, Floirac, France*

³ *Univ. Bordeaux, ISM, UMR 5255, F-33400 Talence, France*

⁴ *CNRS, ISM, UMR 5255, F-33400 Talence, France*

Accepted XXX. Received YYY; in original form ZZZ

ABSTRACT

The ketyenyl radical (HCCO) has recently been discovered in two cold dense clouds with a non-negligible abundance of a few 10^{-11} (compared to H_2) (Agúndez et al. 2015). Until now, no chemical network has been able to reproduce this observation. We propose here a chemical scheme that can reproduce HCCO abundances together with HCO, H_2CCO and CH_3CHO in the dark clouds Lupus-1A and L486. The main formation pathway for HCCO is the $\text{OH} + \text{CCH} \rightarrow \text{HCCO} + \text{H}$ reaction as suggested by Agúndez et al. (2015) but with a much larger rate coefficient than used in current models. Since this reaction has never been studied experimentally or theoretically, this larger value is based on a comparison with other similar systems.

Key words: astrochemistry – ISM: clouds – ISM: abundances – ISM: molecules

1 INTRODUCTION

Cold dark clouds are assumed to be the most simple type of interstellar sources that can be used to test chemical models before being applied to more complex sources such as protostars and protoplanetary disks (Bergin & Tafalla 2007; Agúndez & Wakelam 2013). The clouds have characteristically low temperatures (below 10 K), they are dense (between a few 10^4 to a few 10^6 cm^{-3}) and are shielded from any source of UV field. There exists however a source of UV photons produced by the emission from excited H_2 produced by electrons originating from the ionization of H_2 by cosmic-ray particles (Prasad & Tarafdar 1983). More than 70 molecular species (neutrals, cations and anions) have now been observed in these objects (Agúndez & Wakelam 2013). HCCO was recently detected by Agúndez et al. (2015) with a non negligible abundance of a few 10^{-11} (compared to H_2); an abundance that they could not reproduce using their model.

To study the formation and destruction of these species, chemical models have been developed considering an increasing number of processes both in the gas-phase and at the surface of the grains where a fraction of these species are believed to be formed (Herbst & van Dishoeck 2009). Such models are based on chemical networks containing chemical reactions with their associated rate coefficients. The networks have been constructed over time mostly driven

by new observations. Over the past few years, we have been revisiting those chemical networks from a chemists point of view, to provide a better description of the underlying processes. (Wakelam et al. 2009; Loison et al. 2012; Daranlot et al. 2012; Loison et al. 2014a,b). In this paper, we present a chemical scheme for the formation and destruction of HCCO in cold dense clouds and compare our results with the observed abundances.

2 CHEMICAL MODELING AND NETWORK

2.1 The NAUTILUS chemical model

The model used to simulate the abundance of HCCO in cold dense clouds is NAUTILUS. This model computes the abundance of molecules and atoms (neutrals but also some species in their cationic or anionic forms) in the gas-phase and also at the surface of interstellar grains. The equations and the chemical processes included in the model are described in earlier papers and we refer to Reboussin et al. (2014).

For the gas-phase, many chemical reactions (including bimolecular and unimolecular processes) are considered based on the kida.uva.2014 chemical network by Wakelam et al. (2015). Interstellar ice is modeled by a one-phase rate equation approximation (Hasegawa et al. 1992): there is no differentiation between the species in the bulk and at the surface. The species from the gas-phase are allowed to physisorb on the surface of interstellar grains. Here, they can diffuse and react. The evaporation processes are: thermal (which are

* E-mail: wakelam@obs.u-bordeaux1.fr

inefficient at dense cloud temperatures), induced by cosmic-rays (following Hasegawa & Herbst 1993), and chemical desorption (as defined by Garrod et al. 2007). Photodesorption has not been introduced in this model because photodesorption induced by cosmic-ray secondary photons was found to be inefficient compared to the chemical desorption mechanism by Wakelam et al. (2014). In addition, Bertin et al. (2012) showed experimentally that photodesorption of few CO layers (i.e. ~ 10) adsorbed on amorphous H₂O was inefficient. Until more experiments are performed on water ices, it is reasonable to assume that molecular photodesorption is only a minor desorption process in dense clouds. Species can diffuse by thermal hopping only with a barrier of $0.5 \times E_D$ (with E_D the species binding energy). Reactions with atomic hydrogen can undergo tunneling using the formalism by Hasegawa et al. (1992). For chemical desorption, i.e. partial desorption of the products due to the exothermicity of the reactions occurring at the surface of the grains, approximately 1% of the products is allowed to desorb. In addition to the usual surface diffusion reactions, we have introduced the complexation and low temperature Eley-Rideal mechanism from Ruaud et al. (2015). The Cosmic-Ray Induced Diffusion mechanism is not included because it does not have any impact on the surface chemistry at high visual extinction (see Reboussin et al. 2014).

To simulate the chemistry of dense clouds, the model is used with homogeneous conditions and integrated over 10^7 yrs. The gas is initially composed of atoms (partly ionized depending on the ionization potential of the atoms). The abundances are the same as in Hincelin et al. (2011). For fluorine, not included in Hincelin et al., we use the depleted value of 6.68×10^{-9} (compared to the total proton density) from Neufeld et al. (2005). The C/O elemental ratio is the subject of considerable debate and is of crucial importance for the modeling of dense clouds (Hincelin et al. 2011). For our standard model, we have used a C/O ratio of 0.7 (i.e. the oxygen elemental abundance is 2.4×10^{-4}). The model was run with a dust and gas temperature of 10 K, a total proton density of $2 \times 10^4 \text{ cm}^{-3}$, a cosmic-ray ionization rate of $1.3 \times 10^{-17} \text{ s}^{-1}$, and a visual extinction of 30.

2.2 Modification of the network

The initial gas-phase network is `kida.uva.2014` Wakelam et al. (2015). The network for surface reactions and gas-grain interactions is based on the one from Garrod et al. (2007) with several additional processes from Ruaud et al. (2015). The HCCO molecule was introduced by Ruaud et al. but was not discussed in their paper since it was mostly an intermediate to the formation of more complex species on the surface. Indeed, the gas-phase reactions involving this species were very limited and as we will show in the next section, the gas-phase abundance of this species was very low at times larger than 10^5 yr. In addition to these reactions (listed in Tables A.1 and A.2 of Ruaud et al. 2015), we have introduced and reviewed reactions involving HCCO radicals (presented in Table A1) to take into account the most important pathways for the formation and destruction of this species in the gas-phase.

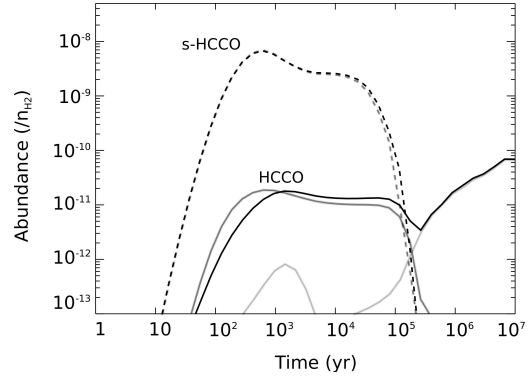


Figure 1. HCCO abundance (with respect to H₂) predicted by our model for typical dense cloud conditions (see section 2.1) as a function of time in the gas-phase (solid lines) and at the surface of the grains (dashed lines). Grey lines show the results obtained with the previous network while the black lines show the results including the new chemistry. The light grey curve for HCCO in the gas phase has been obtained with the new chemistry but removing the reaction $s\text{-CCO} + s\text{-H}$ on the surface.

3 PREDICTED ABUNDANCES

Using the model described above, we have run the simulations with the new chemistry and compared the predictions with the previous results. The HCCO abundance predicted by the model in the gas-phase and at the surface of the grains is shown in Fig. 1. The formation of HCCO on the surface is very efficient between 10^2 and 10^5 yr because of the reaction $s\text{-H} + s\text{-CCO} \rightarrow s\text{-HCCO}$, which is barrier-less for the equivalent gas phase process (Bauer et al. 1985; Schmidt et al. 1983; Horie et al. 1983). $s\text{-CCO}$ is formed through the Eley-Rideal mechanism developed in Ruaud et al. (2015): gas-phase carbon atoms react without a barrier with CO on the ice surface. The absence of a barrier for the $\text{C} + s\text{-CO} \rightarrow s\text{-CCO}$ reaction is deduced from the study of Husain & Kirsch (1971) and ab-initio calculations performed by Ruaud et al. (2015). The gas-phase abundance of HCCO before 10^5 yr is then the result of the chemical desorption (see section 2.1) of $s\text{-HCCO}$ during its formation on the surface. The abundance of HCCO in the gas-phase predicted by the new model without this reaction is also shown in Fig. 1. Note that in Table B1 of Ruaud et al. (2015) only the channel leading to $s\text{-HCCO}$ is indicated but the chemical desorption channel was also included.

After 10^5 yr, its abundance decreases in the previous model because $s\text{-HCCO}$ is also hydrogenated to give $s\text{-H}_2\text{CCO}$ and we did not have any efficient gas-phase formation processes. With the new chemistry, its abundance in the gas-phase increases at larger times. The main production reaction is $\text{OH} + \text{CCH} \rightarrow \text{HCCO} + \text{H}$ as already suggested by Agúndez et al. (2015). There are no theoretical or experimental studies of this reaction. Agúndez et al. used a rate coefficient of $3 \times 10^{-11} \text{ cm}^3 \text{ s}^{-1}$ based on Frenklach et al. (1992). This value is however simply an estimation and there is no justification in Frenklach et al. (1992) of this choice. Based on similar systems, i.e. the $\text{O} + \text{CCH}$ rate constant (Boullart et al. 1996; Devriendt et al. 1996; Devriendt & Peteers 1997; Georgievskii & Klippenstein 2011) or $\text{OH} +$ radicals reactions (De Avillez Pereira et al. 1997; Jasper et al. 2007;

Sangwan et al. 2010), we propose the use of a larger rate coefficient of $2 \times 10^{-10} \text{ cm}^3 \text{ s}^{-1}$. This rate constant is close to the capture rate dominated at low temperature by dipole-dipole interactions and to the one precisely computed by Georgievskii & Klippenstein (2011) for $\text{O} + \text{CCH}$. The rate constant calculation methodology has been described in detail in Loison et al. (2014a).

In this case, the formation of HCCO is faster than its destruction through reactions with H , O and H_3^+ . There is also another potential source of HCCO radicals: the $\text{CCH} + \text{O}_2$ reaction. The rate constant of this reaction is high at low temperature (Chastaing et al. 1998; Vakhtin et al. 2001) and HCCO has been experimentally identified as one of the products (Lange & Gg. Wagner 1975) with a non-negligible branching ratio between 20% to 40% (Lange & Gg. Wagner 1975; Laufer & Lechleider 1984). The production of HCCO radicals is also suggested from theoretical calculations (Sumathi et al. 1998; Li et al. 2004). However in the Lange & Gg. Wagner (1975) and Laufer & Lechleider (1984) studies, the rate constant of the $\text{CCH} + \text{O}_2$ reaction was underestimated and the rate constant of the $\text{HCCO} + \text{O}_2$ reaction was overestimated leading to a large uncertainty in the HCCO product branching ratio. Moreover our current astrochemical model leads to an O_2 abundance higher than observed for dense molecular clouds (Pagani et al. 2003), inducing an overestimation of HCCO production through the $\text{CCH} + \text{O}_2$ reaction. Instead of including HCCO production from the $\text{CCH} + \text{O}_2$ reaction in our standard model (the $\text{CCH} + \text{O}_2$ reaction producing only H , HCO , CO and CO_2 Su et al. 2000), we performed a test run to see the effect of its inclusion. When the $\text{CCH} + \text{O}_2 \rightarrow \text{HCCO} + \text{O}$ reaction is included, an increase of the HCCO abundance is observed in the $3\text{--}5 \times 10^5 \text{ yr}$ range (reaching few 10^{-11} of H_2) corresponding to the peak of the O_2 abundance profile.

Fig. 2 shows the abundances of HCO, H_2CCO and CH_3CHO predicted by our new model as a function of time for the physical conditions described in section 2.1. Compared to Agúndez et al. (2015), H_2CCO is predicted to be much less abundant very likely because we have introduced its destruction reaction with atomic carbon with a rate coefficient of $3 \times 10^{-10} \text{ cm}^3 \text{ s}^{-1}$ (see Ruaud et al. 2015). Our predicted CH_3CHO abundance is quite different from the one of Agúndez et al. (2015) with the UMIST RATE12 or the kida.uva.2014 networks. The difference with their results using the kida.uva.2014 network is mainly due to the fact that they do not consider reactions at the surface of the grains. In our present simulation, CH_3CHO is produced in the gas phase through the $\text{O} + \text{C}_2\text{H}_5$ reaction, C_2H_5 being efficiently produced through surface reactions (mainly $s\text{-H} + s\text{-C}_2\text{H}_4 \rightarrow \text{C}_2\text{H}_5$). The difference between the gas phase models of Agúndez et al. (2015) using the two networks is more complex to analyse. One main difference though between our network and UMIST RATE12 is the inclusion of destruction reactions with atomic carbon.

4 COMPARISON WITH OBSERVATIONS

HCCO has only been observed in two dark clouds, Lupus-1A and L483 by Agúndez et al. (2015) with an abundance of a few 10^{-11} compared to H_2 . These authors also give

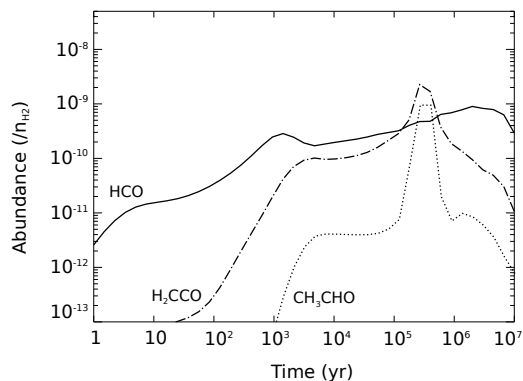


Figure 2. HCO, H_2CCO and CH_3CHO abundances (with respect to H_2) predicted by our model using the new chemistry for the typical dense cloud conditions described in section 2.1 as a function of time in the gas-phase.

upper limits in three other cold sources with a very strong limit for L1521F of 7×10^{-13} . They also detected HCO, H_2CCO and CH_3CHO in the same sources. We will compare our model results with the abundances listed in Table 2 of Agúndez et al. (2015) keeping in mind the uncertainties in the H_2 column densities in these sources (see Agúndez et al. 2015, for discussion). In TMC-1, HCCO was not detected and an upper limit of 2.9×10^{-12} (compared to H_2) was derived by Turner & Sears (1989). The reanalysis of the HCCO observation by Agúndez et al. (2015) gave an upper limit of 5×10^{-11} .

For all the molecules (Figs. 1 and 2), we are able to reproduce reasonably well the observed abundances for times between 10^5 and 10^6 yr (chemical ages usually assumed for dark clouds). Only HCO is slightly overproduced by our model. It is interesting to note that the predicted HCO abundance presents a smooth increase while H_2CCO and in particular CH_3CHO have peak abundances around $2 \times 10^5 \text{ yr}$. This peak abundance of H_2CCO is ten times larger than the observed one in any source. The strong increase of H_2CCO and CH_3CHO near 10^5 yr is due to the fact that these closed shell molecules react only with C atoms and not with H , O or N atoms; the carbon atom abundance strongly decreasing between 10^5 and $2 \times 10^5 \text{ yr}$. The relatively stable abundance of HCO with time may explain the uniform abundance of this molecule observed by Agúndez et al. (2015) in all sources. The main production and destruction reactions for those molecules are summarized in Table B1.

The observed sources present some variations in density and temperature that may influence the chemistry (see Agúndez et al. 2015, and references therein). To test this, we have run our model with a larger total proton density ($n_{\text{H}} = n(\text{H}) + n(\text{H}_2)$) of 2×10^5 and even $2 \times 10^6 \text{ cm}^{-3}$ (see Fig. 3), keeping the other parameters similar to the ones described in section 2.1. As a general result of more collisions, the predicted gas-phase abundances are increased earlier but the peak abundances and late time abundances are smaller because of more efficient depletion on the grains. If some of the sources are denser such as Lupus-1A and L1521F, it is very likely that they have not been that dense for a long period of time. Some of the sources may also be slightly warmer than the typical 10 K usually assumed. We have run our model with gas and grain temperatures of 15 and 20 K (see Fig. 3).

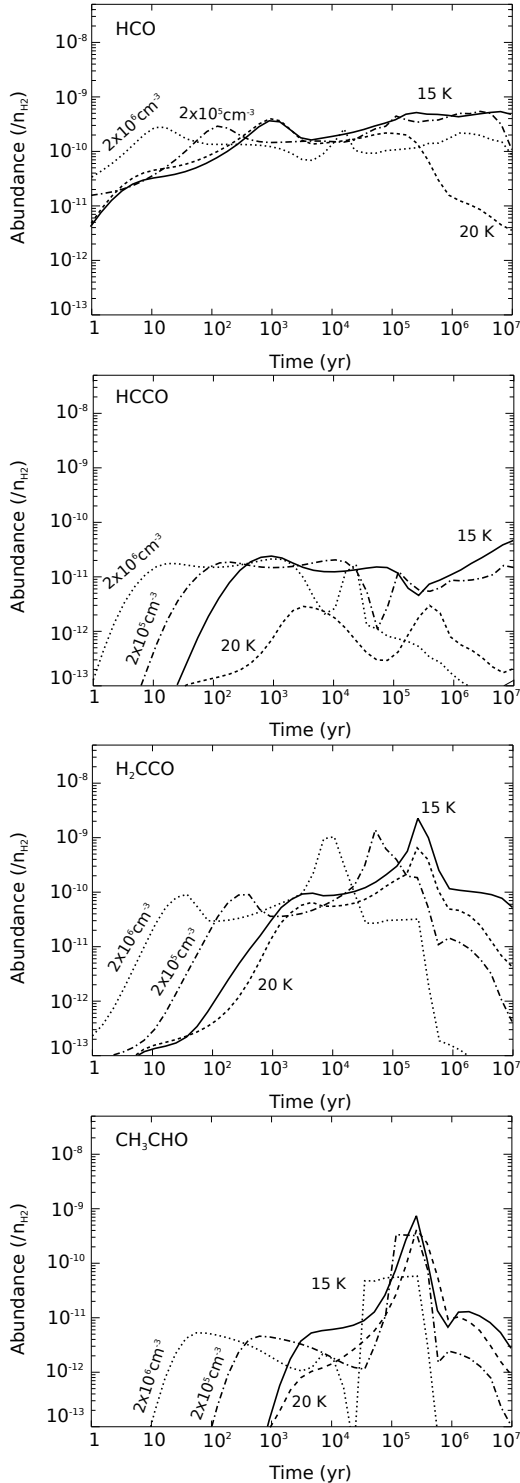


Figure 3. HCO, HCCO, H₂CCO and CH₃CHO abundances (with respect to H₂) predicted by our model using the new chemistry as a function of time in the gas-phase. Some of the physical parameters have been changed compared to the standard model: the gas and dust temperature is set to 15 K for the solid lines and to 20 K for the dashed lines (keeping the H density to $2 \times 10^4 \text{ cm}^{-3}$); the density was set to $2 \times 10^5 \text{ cm}^{-3}$ for the dotted-dashed lines and to $2 \times 10^6 \text{ cm}^{-3}$ for the dotted lines (keeping the temperature to 10 K).

The 15 K model is not very different from the 10 K standard model. In contrast, the 20 K model produces fewer molecules in general except for CH₃CHO which remains relatively unaffected. After 10^5 yr, the 20 K regime is characterized by a smaller abundance of CCH and C₂H₃, a smaller abundance of CO onto the grain surfaces (the evaporation temperature of CO being around 18 K), a larger abundance of atomic hydrogen in the gas-phase, and an increase of the diffusion rate of heavy radicals onto the surface. Before 10^5 yr, less HCCO is produced because of a smaller abundance of CO on the grains (less CCO is formed). After 10^5 yr, it is the larger gas-phase abundance of atomic hydrogen that destroys HCCO efficiently in the gas-phase. The lower abundance of HCCO in the ices leads to less H₂CCO in the gas-phase.

Using an approach similar to Loison et al. (2014a) to compare the HCO, HCCO, H₂CCO and CH₃CHO observed and modeled abundances obtained with the standard physical model, we have found that the observed abundances in Lupus-1A and L483 are best reproduced at 1.8×10^5 yr with a mean difference between observed and modeled abundances of less than a factor of 3. Using a gas and dust temperature of 15 K, the best mean agreement is smaller than a factor of 2 at 1.1×10^5 yr because HCCO and H₂CCO are better reproduced. Considering both the uncertainties in the observations and the chemical modeling, this difference between the models is however insignificant. The "best age" that we give here is only based on the comparison between the modeled and observed abundances of the four molecules. In addition, estimating an age for such sources requires us to define the time zero as a starting point. The formation of dense clouds is a continuous process from the diffuse medium. The formation of molecules is likely to start early on during this process when the density and the visual extinction are smaller than the ones considered in our model. For these reasons, this age should only be considered as the best time in our model to reproduce the observations.

ACKNOWLEDGEMENTS

The authors thank the following funding agencies for their partial support of this work: the French CNRS/INSU programme PCMI and the ERC Starting Grant (3DICE, grant agreement 336474).

REFERENCES

- Agúndez M., Wakelam V., 2013, *Chemical Reviews*, **113**, 8710
 Agúndez M., Cernicharo J., Guélin M., 2015, *A&A*, **577**, L5
 Bauer W., Becker K., Meuser R., 1985, *Ber. Bunsenges. Phys. Chem.*, **89**, 340
 Baulch D. L., et al., 2005, *J. Phys. Chem. Ref. Data*, **34**, 757
 Bergin E. A., Tafalla M., 2007, *ARA&A*, **45**, 339
 Bertin M., et al., 2012, *Phys. Chem. Chem. Phys.*, **14**, 9929
 Boullart W., Devriendt K., Borms R., Peeters J., 1996, *J. Phys. Chem.*, **100**, 998
 Chastaing D., James P. L., Sims I. R., Smith I. W. M., 1998, *Faraday Discuss.*, **109**, 165
 Daranlot J., Hincelin U., Bergeat A., Costes M., Loison J.-C., Wakelam V., Hickson K. M., 2012, *PNAS*, **109**, 10233
 De Avillez Pereira R., Baulch D. L., Pilling M. J., Robertson S. H., Zeng G., 1997, *J. Phys. Chem. A*, **101**, 9681
 Devriendt K., Peeters J., 1997, *J. Phys. Chem. A*, **101**, 2546

- Devriendt K., Van Look H., Ceursters B., Peeters J., 1996, *Chem. Phys. Lett.*, **261**, 450
- Frenklach M., Wang H., Rabinowitz M. J., 1992, *Prog. Energy Combust. Sci.*, **18**, 47
- Garrod R. T., Wakelam V., Herbst E., 2007, *A&A*, **467**, 1103
- Georgievskii Y., Klippenstein S. J., 2011, in Cernicharo J., Bachiller R., eds, IAU Symposium Vol. 280, IAU Symposium. pp 372–382, doi:10.1017/S1743921311025129
- Glass G. P., Kumaran S. S., Michael J. V., 2000, *J. Phys. Chem. A*, **104**, 8360
- Hasegawa T. I., Herbst E., 1993, *MNRAS*, **261**, 83
- Hasegawa T. I., Herbst E., Leung C. M., 1992, *ApJS*, **82**, 167
- Herbst E., van Dishoeck E. F., 2009, *ARA&A*, **47**, 427
- Hincelin U., Wakelam V., Hersant F., Guilloteau S., Loison J. C., Honvault P., Troe J., 2011, *A&A*, **530**, A61
- Horie O., Bauer W., Meuser R., Schmidt V. H., Becker K. H., 1983, *Chemical Physics Letters*, **100**, 251
- Husain D., Kirsch L. J., 1971, *J. Chem. Soc. Faraday Trans.*, **67**, 2025
- Jasper A. W., Klippenstein S. J., Harding L. B., Ruscic B., 2007, *J. Phys. Chem. A*, **111**, 3932
- Lange W., Gg. Wagner H., 1975, *Berichte der Bunsengesellschaft für physikalische Chemie*, **79**, 165
- Laufer A. H., Lechleider R., 1984, *J. Phys. Chem.*, **88**, 66
- Li L., Deng P., Tian A., Xu M., Wong N.-B., 2004, *J. Phys. Chem. A*, **108**, 4428
- Loison J.-C., Halvick P., Bergeat A., Hickson K. M., Wakelam V., 2012, *MNRAS*, **421**, 1476
- Loison J.-C., Wakelam V., Hickson K. M., Bergeat A., Mereau R., 2014a, *MNRAS*, **437**, 930
- Loison J.-C., Wakelam V., Hickson K. M., 2014b, *MNRAS*, **443**, 398
- Neufeld D. A., Wolfire M. G., Schilke P., 2005, *ApJ*, **628**, 260
- Pagani L., et al., 2003, *A&A*, **402**, L77
- Prasad S. S., Tarafdar S. P., 1983, *ApJ*, **267**, 603
- Reboussin L., Wakelam V., Guilloteau S., Hersant F., 2014, *MNRAS*, **440**, 3557
- Ruaud M., Loison J. C., Hickson K. M., Gratier P., Hersant F., Wakelam V., 2015, *MNRAS*, **447**, 4004
- Sangwan M., Chesnokov E. N., Krasnoperov L. N., 2010, *J. Phys. Chem. A*, **116**, 8661
- Schmidt V. H., Meuser R., Horie O., Bauer W., Becker K. H., 1983, *Bull. Soc. Chim. Belg.*, **92**, 655
- Su H., Yang J., Ding Y., Feng W., Kong F., 2000, *Che. Phys. Lett.*, **326**, 73
- Sumathi R., Peeters J., Nguyen M. T., 1998, *Chem. Phys. Lett.*, **287**, 109
- Turner B. E., Sears T. J., 1989, *ApJ*, **340**, 900
- Vakhtin A. B., Heard D. E., Smith I. W. M., Leone S. R., 2001, *Chem. Phys. Lett.*, **344**, 317
- Wakelam V., Loison J.-C., Herbst E., Talbi D., Quan D., Caralp F., 2009, *A&A*, **495**, 513
- Wakelam V., et al., 2012, *ApJS*, **199**, 21
- Wakelam V., Vastel C., Aikawa Y., Coutens A., Bottinelli S., Caux E., 2014, *MNRAS*, **445**, 2854
- Wakelam V., et al., 2015, *ApJS*, **217**, 20

APPENDIX A: LIST OF ADDED REACTIONS

APPENDIX B: MAIN FORMATION AND DESTRUCTION PATHWAYS

This paper has been typeset from a $\text{\TeX}/\text{\LaTeX}$ file prepared by the author.

Table A1. List of gas-phase reactions added to the model and associated parameters.

	Reaction	ΔE (kJ/mol)	α	β	γ	F_0	g	Reference
1	H + HCCO → CH ₂ + CO	-113	1.7×10^{-10}	0.17	0	1.6	0	1,2
2	C ⁺ + HCCO → C ₂ H ⁺ + CO	-411	2.0×10^{-9}	0	0	3	0	3
	→ HCCO ⁺ + C	-143	2.0×10^{-9}	0	0	3	0	3
3	C + HCCO → CCH + CO	-437	2.0×10^{-10}	0	0	3	0	4
4	N + HCCO → HCN + CO	-624	2.0×10^{-11}	0.17	0	3	10	5
	→ HNC + CO	-569	1.0×10^{-11}	0.17	0	3	10	5
	→ NCCO + H	-220	4.0×10^{-11}	0.17	0	3	10	5
5	O + HCCO → H + CO + CO	-428	1.6×10^{-10}	0	0	1.6	0	2
	→ CH + CO ₂	-221	4.9×10^{-11}	0	560	2	100	2
6	OH + CCH → HCCO + H	-220	2.0×10^{-10}	0	0	3	0	3
	→ CH + CO + H	+96	0	0	0	3	0	3
7	HCCO + H ₃ ⁺ → H ₂ CCO ⁺ + H ₂	-387	1.0	3.1×10^{-9}	2.8	2	0	6
8	HCCO + H ₃ O ⁺ → H ₂ CCO ⁺ + H ₂ O	-122	1.0	1.4×10^{-9}	2.8	2	0	6
9	HCCO + HCO ⁺ → H ₂ CCO ⁺ + CO	-244	1.0	1.3×10^{-9}	2.8	2	0	6
10	HCCO + N ₂ H ⁺ → H ₂ CCO ⁺ + N ₂	-339	1.0	1.3×10^{-9}	2.8	2	0	6
11	H ₂ CCO ⁺ + e ⁻ → CH ₂ + CO	-607	2.0×10^{-7}	-0.5	0	3	0	
	→ H + HCCO	-495	1.0×10^{-8}	-0.5	0	3	0	
	→ H + CH + CO	-178	1.0×10^{-7}	-0.5	0	3	0	
	→ H + H + CCO	-92	0	0	0	3	0	
12	CH ₃ CO ⁺ + e ⁻ → CH ₃ + CO	-629	1.0×10^{-7}	-0.5	0	3	0	
	→ H + H ₂ CCO	-509	1.0×10^{-7}	-0.5	0	3	0	
	→ H + CH ₂ + CO	-185	1.0×10^{-7}	-0.5	0	3	0	
	→ H + H + HCCO	-72	0	0	0	3	0	

ΔE is the enthalpy of reaction.

α, β, γ are the parameters to compute the temperature dependent rate coefficients. The Arrhenius-Kooij formula described in Wakelam et al. (2012) should be used for the reactions except for reactions 7 to 10 for which the ionpol1 formula from the KIDA database (<http://kida.obs.u-bordeaux1.fr>) should be used (see also Wakelam et al. 2012). The rates can be used for temperatures between 10 and 300 K.

F_0 and g are parameters used to describe the temperature dependent uncertainty in the rate coefficient (see Wakelam et al. 2012).

References:

1 Glass et al. (2000)

2 Baulch et al. (2005)

3 Close to capture rate

4 Estimation considering the well known reactivity of carbon atoms

5 Reaction on triplet surface with some spin orbit crossing. Part of the HCN should lead to HNC considering the available energy. The last channel was removed because NCCO is not in KIDA.

6 Capture rate

Table B1. Main reactions of production and destruction for HCO, HCCO, H₂CCO and CH₃CHO for two different times and using the new model.

10 ⁴ yr		
Species	Formation	Destruction
HCO	O + CH ₂ → H + HCO O + C ₂ H ₄ ⁺ → HCO + H ₃ ⁺	H + HCO → CO + H ₂ C + HCO → CH + CO / H + CCO
HCCO	s-H + s-CCO → HCCO	O + HCCO → H + CO + CO C + HCCO → CCH + CO
H ₂ CCO	O + C ₂ H ₃ → H ₂ CCO + H s-H + s-HCCO → H ₂ CCO	C + H ₂ CCO → C ₂ H ₂ + CO
CH ₃ CHO	O + C ₂ H ₅ → H + CH ₃ CHO	C + CH ₃ CHO → C ₂ H ₄ + CO
10 ⁶ yr		
Species	Formation	Destruction
HCO	s-H + s-CO → HCO H ₂ COH ⁺ + e ⁻ → H + H + HCO	H + HCO → CO + H ₂
HCCO	OH + CCH → HCCO + H	H + HCCO → CH ₂ + CO
H ₂ CCO	O + C ₂ H ₃ → H + H ₂ CCO	H ₃ ⁺ + H ₂ CCO → H ₂ + CH ₃ CHOH ⁺
CH ₃ CHO	s-H + s-CH ₃ CO → CH ₃ CHO	H ₃ ⁺ + CH ₃ CHO → H ₂ + CH ₃ CHOH ⁺